

ForceCtrl: Hand-Raycasting with User-Defined Pinch Force for Control-Display Gain Application

Seo Young Oh, Junghoon Seo, Juyoung Lee, Boram Yoon, Sang Ho Yoon, and Woontack Woo

Abstract—We present ForceCtrl, a novel 3D hand raycasting technique that enhances pointing precision based on control-display (CD) gain controlled with user-defined pinch force. We introduce a target-agnostic approach for refining raycasting precision, overcoming limitations in human motor accuracy. User-defined pinch force, detected with surface electromyography (sEMG), enables users to easily activate or deactivate CD gain during interaction. We propose three CD gain strategies and compare them through target selection and placement tasks. Our system reduces selection errors, placement jitters, and user workload, especially for distant targets in high-difficulty tasks. These results highlight the effectiveness of applying CD gain to hand raycasting and demonstrate the potential of user-defined pinch force as a robust input modality for precise hand interaction in AR/VR.

Index Terms—Hand Interaction, Force-based Interaction, Virtual and Augmented Realities, Input Accuracy, Raycasting

I. INTRODUCTION

RECENT advances in graphics and display technologies in Augmented Reality (AR) and Virtual Reality (VR) have enabled the visualization of complex 3D environments, often populated with small and densely packed targets. As users increasingly interact with such complicated spatial data, the need for accurate and robust pointing techniques becomes critical for both productivity and user experience. While previous approaches have attempted to reduce interaction complexity by controlling the density or layout of 3D content [1], [2], this strategy is unsuitable in professional domains such as computer-aided design or data visualization, where arbitrary rearrangement hinders interpretation and workflow efficiency.

between physical and virtual interactions are needed, as it does not rely on a handheld device. However, raycasting is greatly affected by human motor abilities [4] and tracking quality [5], [6], making it less suitable for high-precision tasks. To improve interaction with complex 3D environments, we focus on two key challenges: 1) enhancing raycasting precision and 2) enabling precision control without handheld devices.

Several techniques have been proposed to improve ray-based selection, such as object rating systems [7], [8] and pointing prediction models [9]–[11]. While effective in specific contexts, these methods often depend on specific targets or remain limited by human motor accuracy, reducing their generalizability. To address these issues, we introduce a target-agnostic pointing refinement method by applying control-display (CD) gain to the ray itself, reducing sensitivity to fine motor noise. Drawing from the concept of CD ratio in previous 2D and 3D interaction techniques, we define and compare three strategies for applying CD gain to raycasting.

Although bare-hand interaction offers significant advantages over device-based interactions as it preserves natural hand movement, it faces challenges due to limited input modalities. While gaze-based input is often paired with hand interaction [12], [13], it is less effective for rapid mode switching and small targets [14], [15]. To augment hand raycasting without introducing physical constraints, we leverage a familiar selection trigger such as a pinch gesture and measure its intensity using surface electromyography (sEMG). Unlike prior force-based systems that rely on fixed force thresholds [16], [17], our approach utilizes user-defined force levels based on a subjective scale [18], allowing force-based input that accounts for individual differences in force exertion and perception.

We present ForceCtrl, a novel 3D input technique that enables users to control the CD ratio of hand raycasting through user-defined pinch force. Our goal is to enhance the scalability of hand raycasting to better support the growing diversity of tasks in AR/VR environments. By leveraging pinch force, ForceCtrl provides unobtrusive control of the CD ratio, without requiring disruptive gestures or interrupting ongoing pointing tasks. In the following sections, we introduce user-defined pinch force as a robust input modality for interaction state control (Fig. 1(a)), and propose three CD gain strategies to refine ray precision (Fig. 1(b)). We demonstrate that ForceCtrl improves the pointing performance in high-precision tasks, and reveal the benefits of ray convergence and the drawbacks of visual discontinuity across different CD gain strategies. These findings contribute to advancing 3D interaction techniques for complex AR/VR environments and encouraging its adoption in professional and high-precision use cases.

Raycasting is one of the most widely adopted pointing techniques in AR/VR, particularly effective for selecting out-of-reach targets [3]. Among its variants, hand raycasting is especially valuable in scenarios where seamless transitions

Seo Young Oh and Juyoung Lee are with KAIST UVR Lab., Daejeon 34141, Republic of Korea. E-mail: {oh.seo | ejuyoung}@kaist.ac.kr.

Junghoon Seo and Sang Ho Yoon are with KAIST HCI Tech Lab., Daejeon 34141, Republic of Korea. E-mail: {jhseo | sangho}@kaist.ac.kr.

Boram Yoon is with KAIST KI-ITC ARRC., Daejeon 34141, Republic of Korea. E-mail: boram.yoon1206@kaist.ac.kr.

Woontack Woo is with KAIST UVR Lab and KAIST KI-ITC ARRC., Daejeon 34141, Republic of Korea. E-mail: wwoo@kaist.ac.kr

This work was supported partly by National Research Council of Science and Technology (NST) (No. CRC 21011) and partly by Institute of Information & Communications Technology Planning & Evaluation (IITP) (Nos. RS-2024-00397663 and IITP-2025-RS-2022-00156435) grant all funded by the Ministry of Science and ICT (MSIT), Republic of Korea.

This work involved human subjects in its research. Approval of all ethical and experimental procedures and protocols was granted by the KAIST Institutional Review Board under Protocol No. KH2022-130 on December 22, 2023.

(Co-corresponding authors: Sang Ho Yoon and Woontack Woo.)

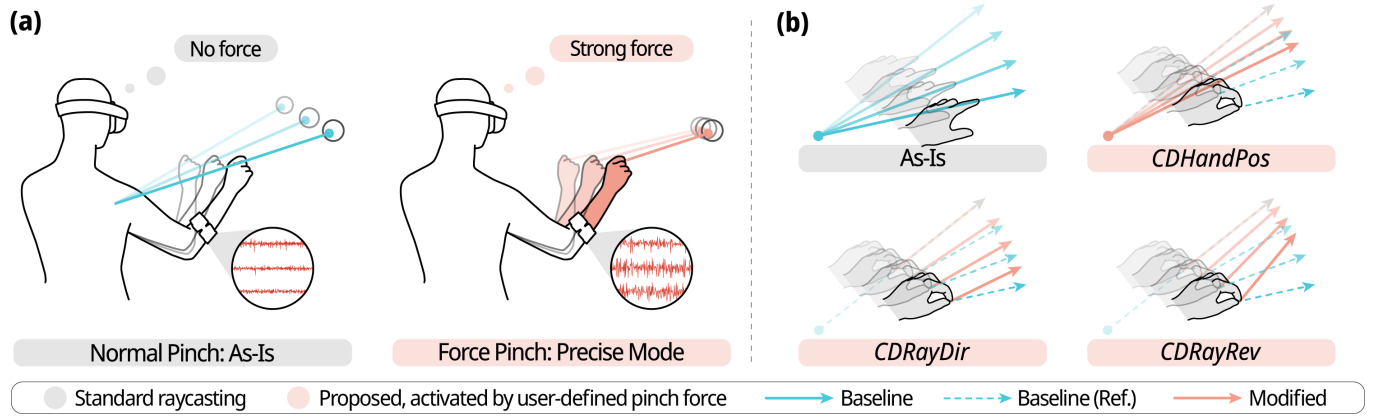


Fig. 1. Overview of ForceCtrl. (a) Users control pointing precision via pinch force detected by an sEMG armband. The ray behaves normally without force and shifts for increased precision when force is applied. (b) We propose and compare three CD gain strategies activated by force: CDHandPos scales hand movement; CDRayDir scales directional change; and CDRayRev applies the scaled directional change in reverse. The strategies are detailed in Section III.C.

II. RELATED WORKS

A. Precise Ray Pointing

As one of the most common 3D interaction methods, raycasting allows users to point and select out-of-reach targets [3]. However, the raycasting method is highly dependent on human motor ability [4], [19], and sensitive to even small movements [20], [21]. Also, ironically, raycasting becomes less accurate at greater distances [22]. Various assistive techniques have been proposed, including expanding selection volume [1], [23], [24], hierarchical disambiguation [25]–[28], and object rating systems [4], [7], [8]. While these methods reduce user's burden of accurate pointing, their reliance on specific targets limits their applicability to other tasks, such as target placement. Although computational models can predict the ray's landing pose [9]–[11], pointing resolution is still confined by human motor limitations.

Applying a CD gain to a pointing method can mitigate the limitations of human motor ability [19], [29]. While CD gain has been used in direct 3D interaction for target selection [2], [30], placement [22], [31], and manipulation [32], its application in distant 3D interaction remains underexplored. Dual-precision pointing [33], or hybrid pointing [34], [35], improves distal pointing accuracy by separating ballistic and corrective phases. However, most mid-air dual-precision techniques are limited to pointers projected on surfaces [36]–[38]. Prior CD gain applications for raycasting have focused on handheld devices [39], [40]. We aim to define a CD ratio for hand raycasting, which differs from handheld raycasting in terms of ray origin and extrapolation.

B. Hand Interactions

Mid-air hand interaction enables natural and expressive interaction for various tasks such as object retrieval [41]–[43] and mode switching [44], [45], without the need for external devices. It is especially well suited for AR, where seamless transitions between virtual and physical contexts are important. Hand raycasting, in particular, has demonstrated performance comparable to handheld controllers given high-quality hand tracking [6], [46]. Although gaze-based interaction presents

a hands-free alternative, its high variability [47], inherent Midas touch problem [48], and limited accuracy for small targets [14], [15] make hand interaction a more reliable choice.

Pinch gestures [20] have been widely studied for their intuitive nature and innate tactile feedback. Often employed as a selection trigger in hand [28], [49], [50] or gaze raycasting [13], [46], [50]–[52], pinch offers fast [53] and temporally precise input [54]. It has also been used for depth control [55], clutching [14], [56], and 3D interaction tasks such as grasping [57], pivoting [58], and bimanual manipulation [12], [59], [60]. However, limiting pinch to binary triggers underutilizes its potential. Recent studies have explored richer input through semi-pinch state [2], [13] or continuous pinch scaling [61]. Building on this, we integrate multiple levels of pinch force, leveraging its natural tactile feedback.

C. Force-based Interactions

Force-based interactions have been widely studied in 2D contexts, particularly in mobile [62] and tabletop settings [63]. These studies have introduced force to enable additional actions [17], [64] or adjust input parameters [16], [65]. In particular, studies that used force or pressure to control input precision [66], [67] suggest its potential to enhance pointing accuracy. In contrast, force-based interactions in 3D has received limited attention. It has mainly focused on mimicking real-world physics [68], [69] and has not been extensively explored as a novel input modality.

The forearm-worn sEMG has long been investigated for hand interactions [70]–[72] due to its non-invasive nature [73]. Although numerous models for sEMG-based finger or pinch force estimation have been proposed, few consider users subjectivity and individual differences. Most models employ direct force regression [69], [74], [75], yielding objective values. Similarly, force level classification typically defines levels based on ground truth force [76] or Maximum Voluntary Contraction (MVC) [77], [78]. Instead, our model classifies user-defined force levels to account for user variability in physical ability and perception.

III. FORCE CLASSIFICATION MODEL

The force classification model forms the foundation of our system, enabling reliable recognition of multiple levels of pinch force to provide explicit control over interaction parameters. The model classifies user-defined pinch force leveraging forearm EMG signals, accommodating individual differences in muscle strength and perception. This section first describes a preliminary study to determine feasible force levels for interaction, followed by the design and evaluation of machine learning models for force classification.

A. Preliminary Study on User-Defined Pinch Force

Our aim is to employ subjectively determined pinch force as a robust input, addressing individual differences in muscle ability and perception. We first validated whether users can distinguish multiple levels of pinching force under a subjective scale. From previously observed correlation between the perceived force intensity and objective measures in hand activities [79], [80], we assumed that the correlation would hold the same for the pinch force exertion.

We recruited 12 participants (7 male, 5 female, ages 22–32, $M = 28.5, SD = 3.37$) with the institutional review board's approval. The participants were equipped with a force sensor (CS8-100N, Singletact) on the thumb. The Borg Category Ratio Scale 10 (Borg Scale) [18], which comprises numbers from 0 to 10, has been commonly used to quantify perceived force intensity by assessing muscle fatigue. We measured four in-between force intensities that are noted with verbal anchors, "2:Weak", "3:Moderate", "5:Strong", and "7:Very Strong", as verbal anchors are the key factor of the scale for quantizing user's experience. We excluded the extremities from the scale, as such force levels are either impractical for repeated execution or less suitable for stable sensing in interaction. We collected 4 trials for each level in a balanced order, obtaining 16 measurements in total. We also captured the MVC of each participant for analysis.

We found a cross-user linear relationship between Borg Scale and %MVC with a regression coefficient of 9.72 ($r^2 = .83, F(1, 238) = 1189, p < .001$). %MVC value was calculated by dividing the measured force by the MVC of the participant in Newtons. The results suggest a common pinch force exertion behavior among participants under the Borg Scale. We also performed a within-participant linear regression, where the regression coefficient ranged in 9.72 ± 0.97 ($r^2 = 0.88 \pm 0.05$). We confirmed users can consistently exert the same pinch force at a given Borg Scale level.

It was also suggested that force levels should be at least three Borg Scale units away from each other to ensure discernibility. For each participant, we compared the four force levels in %MVC. If the measured force intensities of two paired force levels did not make a significant difference, we assumed that the participant did not clearly distinguish the two levels. The result showed that there were 7 participants who were unable to make a significant difference for the "2:Weak" & "3:Moderate" pair, two participants for the "3:Moderate" & "5:Strong" pair, and another two participants for the "5:Strong" & "7:Very Strong" pair. Accordingly, also considering the stability of

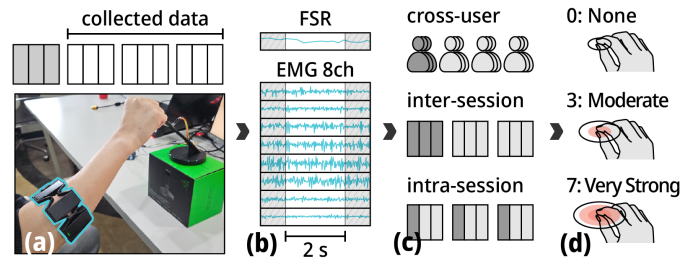


Fig. 2. Force classifier training. (a) Data collection setup and procedure, (b) collected data, (c) training conditions, and (d) classification output.

sEMG signal, we selected "3:Moderate" & "7:Very Strong" pair as the input to our system.

B. Classification of User-Defined Pinch Force

We explored multiple machine learning models to classify the Borg Scale ratings using forearm EMG signals. We recorded forearm EMG signals using an armband with 8 electrodes¹. It should be noted beforehand that our methodologies and findings are not confined to a specific device, and could potentially be extended to alternative EMG-based devices. Data were collected from 12 participants (6 male, 6 female, ages 22–37, $M = 28, SD = 4.92$), at three Borg Scale levels ("0:None", "3:Moderate", "7:Very Strong") across four sessions per participant later excluding the first session (Fig. 2(a)). Each trial involved a 4-second pinch and we analyzed the middle 2 seconds (Fig. 2(b)) yielding 10.8 minutes of data.

We evaluated five distinct models for force classification: logistic regression, a 3-layer neural network, SVM, XGBoost [81], and CNN [69]. We performed tests under three conditions (Fig. 2(c)): cross-user (generalization across users), inter-session (consistency over sessions), and intra-session (performance with session-specific calibration). Participants were split into four groups for cross-user testing, one group for testing and the rest for training, resulting in a 4-fold split. In the inter-session condition, one of three sessions per user was set as test data, forming 36 training-test pairs. For intra-session testing, one of three trials per session was used for testing, creating 108 pairs. The classifier was trained to recognize the three force levels: "0:None", "3:Moderate", "7:Very Strong" (Fig. 2(d)).

In the cross-user condition, the model accuracy ranged from 35.99% to 79.12% with CNN performing best but impractical. In inter-session tests, CNN outperformed logistic regression but showed no significant advantage over SVM and XGBoost in paired t-tests. Pre-training and temporal aggregation improved CNN's median accuracy to 93.35% though still insufficient. In intra-session tests, CNN significantly outperformed all models and reached 99.65% accuracy with pre-training and temporal aggregation. Due to its high intra-session performance, we adopted CNN in our system (Fig. 3(a)).

To address the reliability issues of EMG-based systems from motion noise and equipment problems [73], we added a history accumulator. Our system updates the force level only when

¹Thalmic Labs Myo armband: <https://github.com/thalmiclabs>

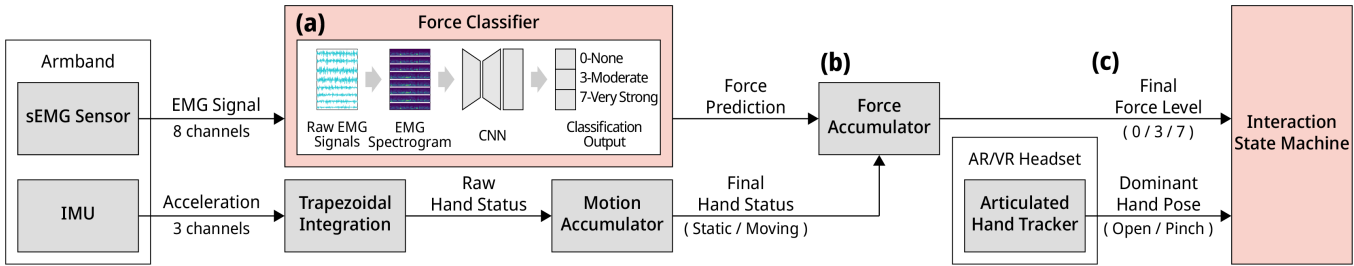


Fig. 3. System architecture of ForceCtrl. (a) A pre-trained CNN processes 8-channel sEMG data and classifies it into three force levels. (b) The output is post-processed with motion data using a history accumulator. (c) The final classification, combined with hand pose, determines the interaction state.

256 the history accumulator is filled with the same class for 60
 257 frames, for both responsiveness and stability (Fig. 3(b)). We
 258 also integrated IMU signals, assuming users would not change
 259 pinch force during rapid hand movements. When hand velocity
 260 exceeds the threshold, the history accumulator does not update.
 261 If the output of the force history accumulator is consistent
 262 over 50 ms, we combine it with the hand pose tracked by the
 263 headset and alter the system's interaction state (Fig. 3(c)). The
 264 interaction state remains unchanged for 0.6 s after a change
 265 to ensure stability. By combining EMG and IMU data with
 266 temporal aggregation, our system improves force classification
 267 reliability.

IV. FORCECTRL SYSTEM

268 ForceCtrl is designed to improve the accuracy of hand
 269 raycasting in a target-agnostic manner, supporting both precise
 270 selection and placement. Built on the force classification
 271 model, it enables explicit control of pointing precision: the
 272 ray becomes more precise as pinching force increases. The
 273 system allows seamless alteration of pointing precision without
 274 disrupting users' workflow.

A. Interaction States

275 Without any force exertion detected by the force classification
 276 model, the system operates as usual, in the same way as
 277 the standard hand raycasting. When the index finger is open,
 278 the pointer is in the coarse pointing state (Fig. 4(a)). When a
 279 pinch gesture is recognized, the pointer turns into the coarse
 280 dragging state, considered to be clicked (Fig. 4(b)).

281 When users require greater pointing accuracy, they can activate
 282 the precise states by applying the pinching force. A force of
 283 "3:Moderate" triggers the precise pointing state (Fig. 4(c)).
 284 In this state, the pointer's movement is damped, as detailed
 285 later in this section, enabling more sensitive control with
 286 the same hand movement. This mapping, where a stronger
 287 pinch results in smaller ray movement, may feel intuitive as
 288 it resembles the metaphor of drag force.

289 Then, the force of "7:Very Strong" triggers the precise
 290 dragging state (Fig. 4(d)). Pointer movement is also damped
 291 in this state. With increased pinching force, users can either
 292 select an object with a brief click or grab it by maintaining
 293 the force. Although the exertion of "7:Very Strong" can be
 294 physically demanding, this state is expected to be held only
 295 briefly in typical use.

B. State Transitions

296 Pinch can activate three different states: coarse dragging,
 297 precise pointing, and precise dragging. Upon detecting a pinch
 298 gesture, the system awaits the next output from the classification
 299 model. If the classified force level is "0:None", coarse
 300 dragging state is activated. A force level of "3:Moderate"
 301 triggers the precise pointing state. No transition occurs when
 302 the force is classified as "7:Very Strong" at the moment of
 303 pinch. Notably, the states are not sequential; although the user
 304 naturally transitions through the intermediate levels, the 50 ms
 305 window systematically allows direct activation of the states.

306 The precise dragging state is only accessible when the
 307 pointer is already in either the coarse dragging or precise
 308 dragging state. Releasing the pinch returns the system to coarse
 309 pointing.

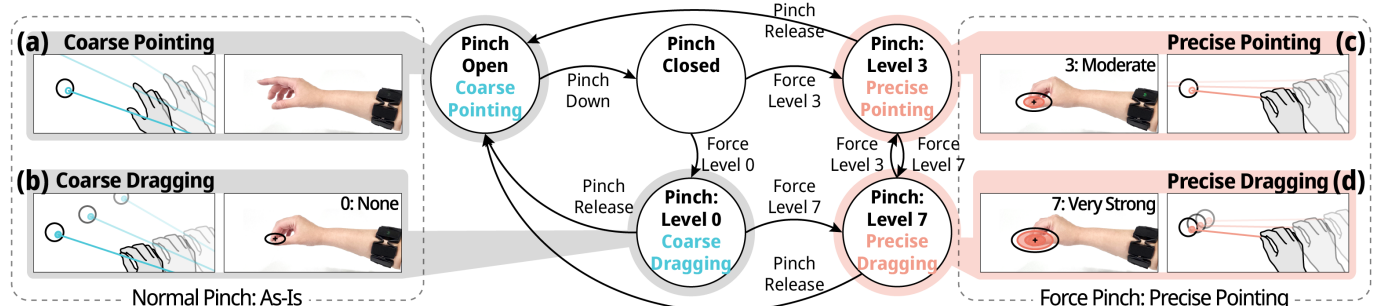


Fig. 4. Interaction state transitions. (a) Coarse pointing, (b) coarse dragging, (c) precise pointing, and (d) precise dragging. Upon a pinch, the system waits for the next force classification and transitions to either coarse dragging or precise pointing. Precise dragging is only reachable from these two. Releasing the pinch returns the system to coarse pointing.

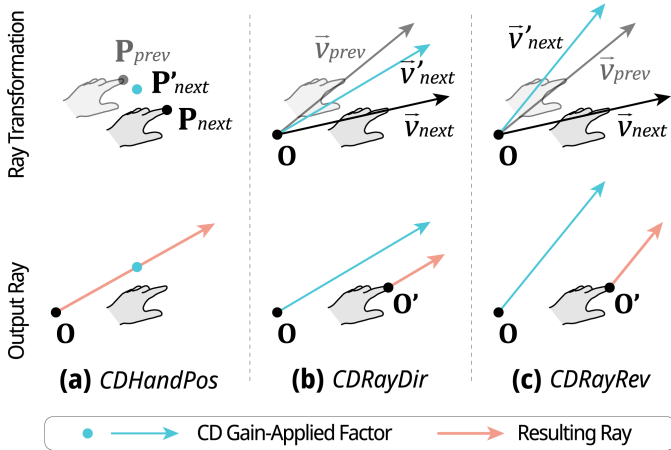


Fig. 5. Three ray shifting strategies. (a) CDHandPos, (b) CDRayDir, (c) CDRayRev. Top row: the ray transformation process to apply CD gain; bottom row: the resulting output ray. P is the hand's position, P' is the CD gain-applied position. \vec{v} is the vector of the pointing ray, \vec{v}' is the CD gain-applied vector. O and O' are the origins of the pointing ray.

311 pointing state. This transition logic assumes that users are
312 unlikely to change both precision and selection state simultaneously.
313 The system allows returning from precise dragging to
314 precise pointing, enabling actions such as consecutive clicks.
315 However, transitioning directly from precise dragging to coarse
316 dragging is not permitted, as we assume users would not
317 attempt to “reset” the pointer mid-drag. Users can always exit
318 to the coarse pointing state by releasing the pinch.

319 C. Ray Shifting

320 While the CD ratio is well defined in 2D pointing, the
321 concept becomes less clear in 3D ray-based pointing, where
322 the ray extends infinitely and lacks a fixed endpoint. To address
323 this, we propose three approaches, each applied to a different
324 component of the ray. To ensure broader applicability, all
325 approaches are designed to be target-agnostic, making them
326 suitable for both target selection and placement tasks. We im-
327 plemented the system using discrete force-based states rather
328 than a continuous force-to-gain mapping to support multiple
329 interaction modes and ensure robust interaction. Discrete states
330 allow four functionally distinct phases, whereas continuous
331 scaling would permit only two: pinching and not pinching.
332 Prior work also showed that implicit transition results in sig-
333 nificantly lower performance and preference for small targets
334 than using a discrete mode switch [36].

335 **CDHandPos.** A straightforward approach is to treat the
336 real hand as the control input and the virtual hand as the
337 display output [2], applying the CD gain to the real hand's
338 translation to determine the virtual hand's position (Fig. 5(a)).
339 Specifically, the 3D displacement of the hand is scaled by the
340 CD gain and added to the virtual hand's previous position:

$$341 P'_{next} = P'_{prev} + (P_{next} - P_{prev}) \times g_{CD}$$
. Likewise, the change in
342 ray direction is scaled and added to the previous ray direction:

$$343 \vec{v}'_{next} = \vec{v}'_{prev} + (\vec{v}_{next} - \vec{v}_{prev}) \times g_{CD}$$
. This effectively extrapolates
344 the ray through the modified hand position. Note that the
345 virtual hand is a conceptual construct and is not rendered to
346 the user. Although simple, this method can cause the ray to

visually detach from the user's hand, potentially leading to dissonance in the user experience.

347 **CDRayDir.** Inspired by prior work that damped rotational
348 changes in handheld raycasting [39], [40], this second ap-
349 proach scales the directional change of the ray (Fig. 5(b)). In
350 this method, the hand position remains unchanged, while the
351 change in ray direction is scaled by the CD gain and applied
352 to the previous direction: $\vec{v}'_{next} = \vec{v}'_{prev} + (\vec{v}_{next} - \vec{v}_{prev}) \times g_{CD}$. This
353 maintains visual continuity between the ray and the hand,
354 reducing the disconnection introduced in the previous method.
355 In terms of the CD ratio, the control input is the change in ray
356 direction, and the display output is the adjusted ray direction.
357 However, as the ray continues to diverge, pointing resolution
358 still decreases with distance, though to a lesser extent.

359 **CDRayRev.** To address not only human motor limitations
360 but also pointing resolution at a distance, we developed a third
361 approach (Fig. 5(c)). Consider a hypothetical target: consistent
362 with the purpose of the CD gain, its movement should follow
363 the user's hand with reduced displacement [22], [31]. To
364 achieve this in a target-agnostic manner, we counteract hand
365 movement by reversing and scaling the directional change of
366 the ray: $\vec{v}'_{next} = \vec{v}'_{prev} - (\vec{v}_{next} - \vec{v}_{prev}) \times g_{CD}$. This causes the
367 ray to gradually converge, reducing the apparent motion of a
368 distant point along the ray. Although the CD gain is applied
369 to the ray direction, this control-display relationship can be
370 interpreted as hand translation (control) resulting in scaled
371 movement of an imaginary target along the ray (display). This
372 results in higher precision as the pointing distance increases.

375 D. Implementation of CD Gain

376 We determined different CD gains for each of the three
377 proposed methods. Previous studies have shown that appro-
378 priate CD gain values for pointing techniques can be derived
379 from the device characteristics and human factors [29], [33].
380 Following these frameworks, we calculated CD gains that do
381 not trigger clutching or precision issues.

382 Device characteristics were based on the technical specifica-
383 tions of the Meta Quest 3², used in our implementation, while
384 human factors were drawn from the literature [82], [83]. We
385 assumed optimal performance of vision-based hand tracking,
386 such that input resolution is limited solely by human motor
387 ability. Additionally, the input device's operating range was
388 assumed to match its field of view (FoV), since visual feedback
389 is lost beyond it regardless of tracking.

390 CD gains were configured to produce an angular resolution
391 between 0.34° to 0.43° at a distance of 2 m with a hand
392 movement of 1.5° . This allows the smallest hand motion
393 to reliably target objects as small as 1° at 2 m, which is
394 considerably small yet clearly visible. The CD gain values for
395 CDHandPos, CDRayDir, and CDRayRev were 0.29, 0.038,
396 and 0.025.

397 V. USER EXPERIMENT

398 We aimed to evaluate the impact of the ForceCtrl system
399 and the three CD-gain-based pointing strategies. To reflect

²Meta Quest 3: <https://www.meta.com/kr/en/quest/quest-3>

400 real-world AR/VR use cases, we adopted object positioning
 401 task [84], following prior work [2], [22]. The task was divided
 402 into two parts—a selection task and a placement task—to
 403 enable separate analysis of objective performance measures.

404 The proposed pointing methods were implemented based on
 405 the raycasting capabilities of the Meta XR Interactions SDK³.
 406 The baseline condition (Baseline) used the SDK's default
 407 raycasting. Surface EMG data were collected using a Thalmic
 408 Labs Myo armband. The interaction system was built on Unity
 409 2021.3.22f1⁴ running on Windows 11. All data collection was
 410 conducted on a PC equipped with an Nvidia GeForce RTX
 411 3090 GPU and an Intel Core i7-11700K CPU, with a Meta
 412 Quest 3 connected via Meta Quest Air Link.

413 A. Experiment Design

414 We recruited 16 participants (8 male, 8 female, 22–33,
 415 $M = 27.6, SD = 3.6$, all right-handed) through the institute's
 416 online community board. All participants self-identified as
 417 intermediate to expert users of hand raycasting in AR/VR;
 418 7 reported moderate experience, 7 used it extensively, and 2
 419 used it daily. The experiment was approved by the institutional
 420 review board and all participants provided their informed
 421 consent. Participants received \$20 for 2 hours of participation.

422 In the selection task, participants were asked to select a
 423 designated target from a group of small, identical spheres. Each
 424 trial presented one target and 48 obstacle spheres distributed
 425 within a 20 cm cube. The target was colored yellow (Fig. 6(a))
 426 and turned blue upon selection (Fig. 6(b)). When pointed
 427 at, spheres were highlighted in cyan. The trial began when
 428 participants selected a “start” sphere and ended when they
 429 released the pinch after correct selection.

430 The placement task required precisely aligning a spherical
 431 target within a cubic goal sized to enclose the sphere. The
 432 target-goal pair appeared at an eccentricity of 10° in the
 433 FoV, with the target on the non-dominant hand side and
 434 the goal on the opposite side. A semi-transparent reference
 435 sphere was displayed inside the cube to assist with accurate
 436 placement (Fig. 6(c)). The target was highlighted in green
 437 upon contact with the goal (Fig. 6(d)). Task completion time
 438 was measured from the first collision with the goal, capturing
 439 only the fine-tuning phase. The trial ended upon release if the
 440 target was in contact with the goal.

441 Both tasks were conducted using a within-subject design
 442 with four **Technique** conditions and two **Depth** conditions.
 443 In the Close condition, targets were placed at a distance of
 444 1.0 m, beyond arm's reach. In the Far condition, depths were
 445 set to 2.0 m for the selection task and 1.5 m for the placement
 446 task, since the latter required higher visual acuity due to its
 447 finer spatial demands. To minimize visual confounding, all
 448 targets were set to 35 mm in diameter, corresponding to 1° of
 449 visual angle at 2 m. While no formal standard exists for the

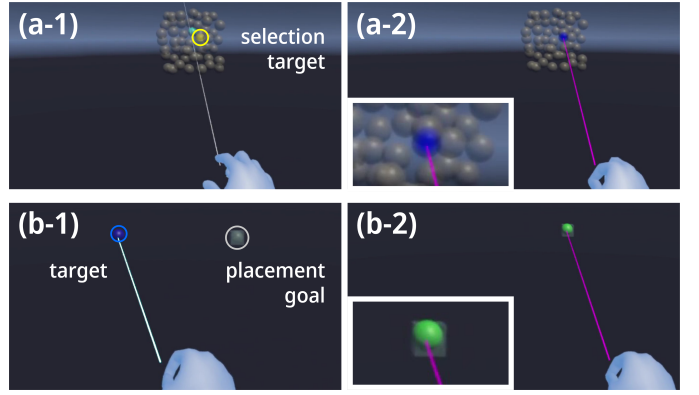


Fig. 6. Experimental tasks. *Selection task*: (a-1) participants select the yellow target; cyan indicates pointing, (a-2) blue indicates correct selection. *Placement task*: (b-1) participants place a target into a cube; (b-2) green indicates successful placement. The colored ray denotes precise states; and thicker ray indicates dragging states.

450 minimum interactable size of virtual objects, we followed the
 451 recommended size of UI buttons in AR⁵ to ensure visibility.

452 We tested four interaction techniques, using standard hand
 453 raycasting as the baseline and comparing it with the three pro-
 454 posed methods. With the Baseline, no force-triggered actions
 455 were available, and only coarse states were used. We altered
 456 line width and color to visualize precision and selection state,
 457 with each proposed technique shown in a distinct color (red,
 458 green, or blue) during precise states. For experimental control,
 459 irrelevant interaction states were deactivated in each task.

460 In addition to task completion time, we recorded selection
 461 errors in the selection task—counting incorrect selections on
 462 obstacles or in empty space—and final offset in the place-
 463 ment task. Subjective responses were collected through post-
 464 condition questionnaires. Perceived workload was assessed
 465 using the NASA Task Load Index (NASA-TLX) [85], with
 466 scores ranging from 0 to 100. Participants also responded
 467 to two 7-point Likert scale items assessing perceived task
 468 performance (Q1: “*I successfully executed the task.*”; Q2: “*I*
 469 *successfully controlled the pointer.*”). In the post-session ques-
 470 tionnaire, participants indicated their most and least preferred
 471 techniques, as well as the techniques they perceived as most
 472 and least accurate.

473 The experiment included a total of 240 trials per partici-
 474 pant. Each task was performed under two **Depth** conditions,
 475 presented in order of distance as the Far condition was more
 476 demanding. Four **Technique** conditions were counterbalanced
 477 across participants. For each **Depth** × **Technique** combination,
 478 participants completed three sets of five trials, with the first
 479 set treated as practice and excluded from analysis. Trials were
 480 timed out after 20 seconds, and participants rested at least 15
 481 seconds between sets to reduce fatigue. Before the main tasks,
 482 participants briefly calibrated the system by exerting each
 483 of three force levels—“0:None”, “3:Moderate”, and “7:Very
 484 Strong”—once, based on the Borg Scale. A short verification
 485 stage followed in which participants tested a series of force
 486 levels. After being introduced to the system, they practiced all

³Meta XR Interactions SDK: <https://developer.oculus.com/downloads/package/meta-xr-interaction-sdk/>

⁴Unity 2021.3.22f1: <https://unity.com/kr/releases/editor/whats-new/2021.3.21>

⁵Buttons—Mixed Reality: <https://learn.microsoft.com/windows/mixed-reality/design/button>

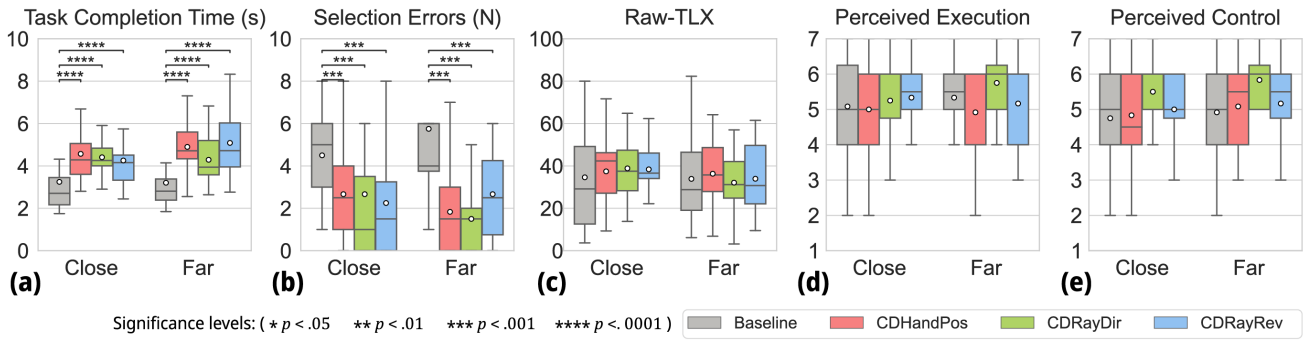


Fig. 7. Selection task results. (a) Task completion time, (b) number of selection errors, (c) Raw-TLX, (d) perceived execution, (e) perceived control.

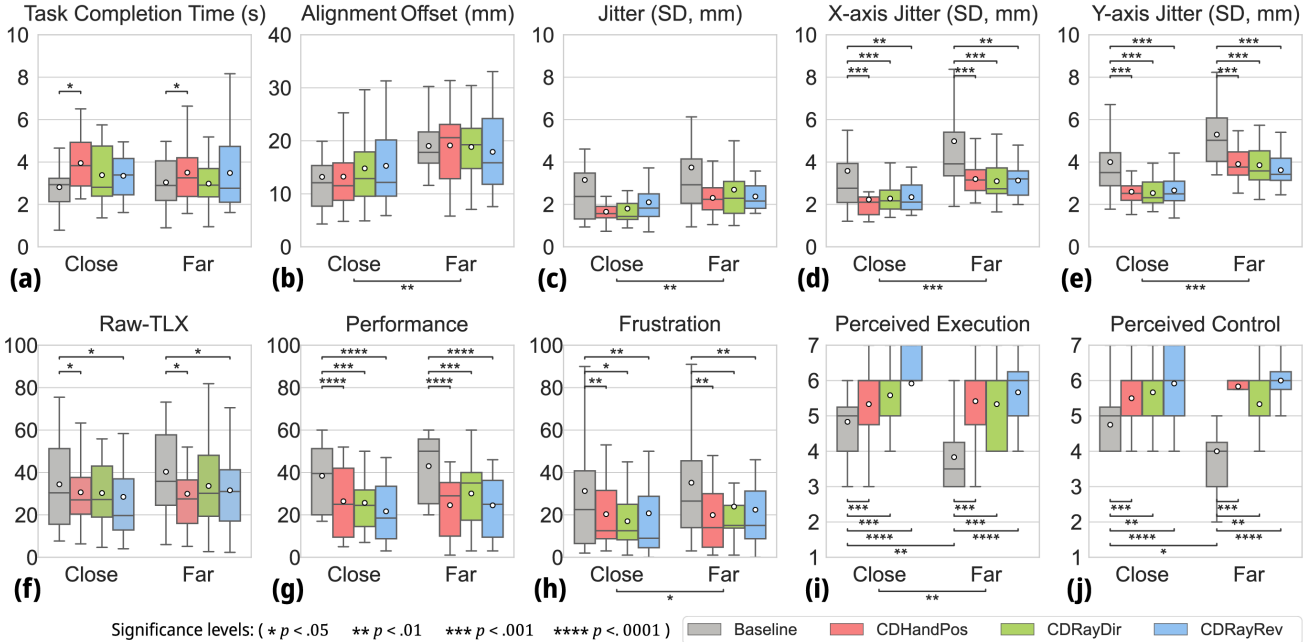


Fig. 8. Placement task results. Top row: objective results. (a) Task completion time, (b) final offset between target and goal, (c) jitter standard deviation, (d) jitter along X-axis, (e) jitter along Y-axis. Bottom row: subjective results. (f) Raw-TLX, (g) performance subscale, (h) frustration subscale, (i) perceived execution, (j) perceived control.

487 four interaction states. During the experiment, participants re-
488 sponded to the NASA-TLX and a post-condition questionnaire
489 every 15 trials. After the selection task, participants completed
490 a post-session questionnaire. The same procedure was repeated
491 for the placement task.

492 B. Quantitative Results

493 For objective measures, we used a two-way repeated
494 measures ANOVA ($\alpha = .05$) after verifying normality with
495 the Shapiro-Wilk test and sphericity with the Mauchly's
496 test. When assumptions were violated, we applied a two-
497 way repeated measures ANOVA using Aligned Rank Trans-
498 form (ART) [86] for non-parametric factorial analysis. All
499 post-hoc pairwise comparisons were corrected using the
500 Benjamini-Hochberg procedure. Subjective measures were
501 analyzed using ART as well. Participants with an extreme
502 number of timed-out trials or selection errors were excluded
503 from the analysis.

504 1) *Selection task*: **Technique** had a significant main effect
505 on task completion time ($F(3,33) = 23.898, p < .001, \eta_p^2 =$
506 $.685$). All ForceCtrl techniques increased completion time
507 compared to the Baseline (all $p < .001$; Fig. 7(a)). **Technique**
508 also significantly affected the number of selection
509 errors ($F(3,33) = 9.715, p < .001, \eta_p^2 = .469$), with Baseline
510 resulting in more frequent incorrect selections than all three
511 ForceCtrl techniques (all $p < .001$; Fig. 7(b)). No significant
512 differences were observed in subjective workload among
513 techniques (Fig. 7(c)–(e)).

514 2) *Placement task*: **Technique** had a significant effect on
515 task completion time ($F(3,33) = 3.370, p = .030, \eta_p^2 = .235$),
516 with CDHandPos requiring more time than Baseline ($p = .023$;
517 Fig. 8(a)). For placement accuracy, measured as the offset
518 between the target and goal, only **Depth** showed a significant
519 main effect ($F(1,11) = 17.674, p = .001, \eta_p^2 = .616$; Fig. 8(b)).

520 We additionally analyzed the target's jitter during the
521 alignment using the standard deviation of the target's
522 position. Although only **Depth** had a significant effect

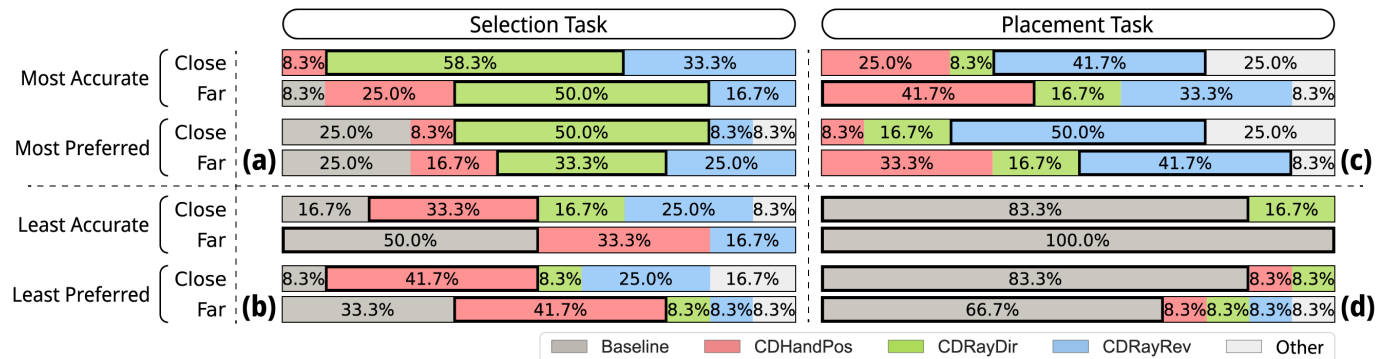


Fig. 9. Qualitative ratings. (a) Positive and (b) negative ratings in the selection task, and (c) positive and (d) negative ratings in the placement task.

on overall jitter ($F(1,11) = 18.965, p = .001, \eta_p^2 = .633$; Fig. 8(c)), **Technique** significantly affected jitter along the X-axis ($F(3,33) = 8.694, p < .001, \eta_p^2 = .441$; Fig. 8(d)) and Y-axis ($F(3,33) = 10.823, p < .001, \eta_p^2 = .496$; Fig. 8(e)). Baseline resulted in greater fluctuations than CDHandPos ($p < .001$), CDRayDir ($p < .001$), and CDRayRev ($p = .001$) on the X-axis, all three techniques (all $p < .001$) in Y-axis. **Depth** also significantly increased jitter along X-axis ($F(1,11) = 70.515, p < .001, \eta_p^2 = .865$) and Y-axis ($F(1,11) = 112.773, p < .001, \eta_p^2 = .911$).

For subjective measures in the placement task, **Technique** had a significant effect on Raw-TLX scores ($F(3,33) = 3.814, p = .019, \eta_p^2 = .257$), with CDHandPos ($p = .034$) and CDRayRev ($p = .022$) reducing perceived workload compared to Baseline (Fig. 8(f)). **Technique** also affected the NASA-TLX performance subscale ($F(3,33) = 16.701, p < .001, \eta_p^2 = .603$) and frustration subscale ($F(3,33) = 5.977, p = .002, \eta_p^2 = .352$). All ForceCtrl techniques were rated as significantly better in performance than Baseline (all $p < .001$; Fig. 8(g)). Baseline resulted higher frustration than CDHandPos ($p = .005$), CDRayDir ($p = .011$), and CDRayRev ($p = .004$). In terms of **Depth**, frustration was significantly higher in the Far condition compared to the Close condition ($F(1,11) = 6.204, p = .030, \eta_p^2 = .361$; Fig. 8(h)).

Perceived task execution, measured on a 7-point Likert scale, was significantly affected by both **Technique** ($F(3,33) = 12.587, p < .001, \eta_p^2 = .534$) and **Depth** ($F(1,11) = 14.533, p = .003, \eta_p^2 = .569$). Participants rated their execution with Baseline significantly lower than with all three ForceCtrl techniques (all $p < .001$). Execution ratings also declined in the Far condition compared to Close. Additionally, a significant interaction between **Technique** and **Depth** was observed ($F(3,33) = 3.704, p = .021, \eta_p^2 = .252$). Perceived execution decreased with depth when using the Baseline technique ($p = .006$; Fig. 8(i)). **Technique** also significantly affected perceived control ($F(3,33) = 12.139, p < .001, \eta_p^2 = .525$), with participants reporting better control with three ForceCtrl techniques than with Baseline (all $p < .001$). A significant interaction between **Technique** and **Depth** ($F(3,33) = 3.245, p = .034, \eta_p^2 = .228$) indicated that perceived control declined with increased depth in the Baseline condition ($p = .036$; Fig. 8(j)).

C. Qualitative Feedback

1) *Selection task*: Participants most frequently rated CDRayDir as the most accurate technique in both Close (58.3%) and Far (50.0%) conditions, followed by CDRayRev in Close condition (33.3%) and CDHandPos in Far condition (25.0%). Regarding preference, CDRayDir was also the most preferred technique in both Close (50.0%) and Far (33.3%) conditions (Fig. 9(a)). For the least accurate ratings, CDHandPos was most frequently selected in the Close condition (33.3%), while Baseline received the highest proportion in the Far condition (50.0%). CDHandPos was again selected most often as least preferred technique (41.7% in both depth conditions), followed by CDRayRev in Close condition (25.0%) and Baseline in Far condition (33.3%) (Fig. 9(b)).

2) *Placement task*: CDRayRev was rated as the most accurate technique in Close (41.7%) condition, while CDHandPos was most often selected in Far condition (41.7%) followed by CDRayRev (33.3%). In terms of preference, CDRayRev was selected most frequently in both Close (50.0%) and Far (41.7%) conditions (Fig. 9(c)). For least accurate, Baseline was most frequently chosen in both Close (83.3%) and Far (100.0%) conditions. CDRayDir was selected as the least accurate in Close condition (16.7%), and the remaining techniques received no votes in either condition. For least preferred, Baseline was selected by the majority of participants in both Close (83.3%) and Far (66.7%) conditions (Fig. 9(d)).

VI. DISCUSSION

The experimental results demonstrate that ForceCtrl enables users to stabilize the pointer for precise interaction with small and distant targets, while maintaining a comparable level of perceived workload. Although the ForceCtrl techniques resulted in slower task completion times, this was expected, as the technique inherently involves an additional step for adjusting the pointer. Importantly, the ForceCtrl techniques reduced frustration and perceived performance difficulty, particularly in high-precision tasks. Based on these results, we discuss three key areas in this section: 1) the feasibility of using user-defined force as an input modality, 2) the implications of applying CD gain to raycasting, and 3) limitations and future directions. Our goal is to provide a comprehensive interpretation of the

607 findings and outline the potential for further development of
608 precise pointing techniques in 3D environments.

609 *1) User-Defined Force as Input:* The results suggest that the
610 performance benefits from our method outweigh the required
611 efforts to perform force-based input. As we used the user-
612 defined values corresponding to “3:Moderate” and “7:Very
613 Strong” as input levels, we anticipated higher physical load
614 in compare to the standard raycasting due to additional force
615 exertion. However, no significant increase in physical demand
616 was observed in either the Raw TLX or its physical demand
617 subscale. At the same time, participants reported reduced
618 frustration and perceived performance difficulty with ForceCtrl
619 techniques. These findings indicate that when users perceive
620 substantial benefits—such as improved pointing accuracy in
621 demanding tasks—they are more willing to accept the physical
622 effort involved.

623 Our findings also show that user-defined force can be
624 generalized across individuals and used as a robust input
625 approach. All 16 participants were able to successfully control
626 the system with only a minimal calibration process, requiring
627 a one-time measurement of three force levels. The system
628 reliably classified users’ subjective force input, demonstrating
629 both the robustness of the model and a common pattern in
630 how users apply force. Moreover, participants were able to
631 exert force consistently throughout the experiment, without
632 noticeable fluctuation or decline over time. These results
633 support the feasibility of user-defined force as a reliable input
634 method for both the user and the system.

635 *2) CD Gain for Hand Raycasting:* While the application
636 of CD gain showed clear advantages over the Baseline
637 technique, among the three proposed methods, CDRayRev
638 with convergence was most preferred in high-difficulty tasks,
639 whereas the visual detachment in CDHandPos negatively
640 impacted user experience. In general, techniques rated highly
641 in accuracy were also commonly rated as the most preferred.
642 As task difficulty increased in the Far condition, differences
643 in perceived performance became more pronounced. Despite
644 all three proposed techniques requiring the same amount of
645 force and offering comparable pointing resolution at the tested
646 depths, participants’ subjective impressions varied consider-
647 ably between techniques.

648 Aligned with the quantitative results, the Baseline technique
649 showed a clear drop in subjective performance as task dif-
650 ficulty increased. While only 16.67% of participants rated
651 Baseline as the least accurate in Close condition of the
652 selection task, 100.00% of participants reported that Baseline
653 was the least accurate in Far condition of the placement
654 task. This disparity highlights its unsuitability for spatially
655 demanding tasks. Participants pointed out that Baseline was
656 “hard to control in high-difficulty tasks” (P16). Specifically,
657 many responded that they had to “put both mental and
658 physical effort to keep my arm steady” and some even “found
659 myself holding my breath” (P14) and “felt frustration” (P16)
660 with Baseline technique.

661 CDRayDir was consistently rated as the most accurate and
662 preferred technique in the selection task, and reported to be
663 “intuitive” (P3) and “natural” (P9). However, in the place-
664 ment task, where higher spatial accuracy is required, both the

665 perceived accuracy and preference of CDRayDir decreased.
666 Participants reported that they were “able to control accuracy
667 without having to move my arm much” (P1), but “had the
668 lowest precision” (P1) at the same time. This indicates that
669 CDRayDir has a relatively subtle effect on precision, making
670 it suitable for moderate-difficulty tasks, but not sufficient for
671 high-difficulty tasks. Consequently, participants did not prefer
672 CDRayDir in the placement task reporting that “it didn’t really
673 feel effective while I still had to apply force” (P15).

674 In contrast, CDRayRev was rated highest in the placement
675 task in both perceived accuracy and preference. Four partic-
676 ipants perceived CDRayRev to be “most accurate” (P2–5),
677 and P4 reported that “it showed significantly less jitter when
678 stationary”. As the placement task required finer control, the
679 convergence of CDRayRev may have helped participants sta-
680 bilize their movements during precise object alignment. While
681 this technique deviates most from the standard raycasting,
682 the technique aligned most closely with participants’ mental
683 model, explicitly supported by six participants. CDRayRev
684 was reported to be “most natural” (P2), “matched my expecta-
685 tion” (P6), and “intuitive” (P4). Since CD gain is intended to
686 reduce pointer movement relative to user input, the conver-
687 ging behavior of CDRayRev may have affected participants’
688 perception of the technique as intuitive.

689 Although CDHandPos received high accuracy ratings es-
690 pecially in the Far condition of the placement task, it was
691 not preferred in general. Some participants highlighted this
692 contrast: “it had the highest precision, but required the most
693 arm movement” (P1), even though the pointing resolutions of
694 three tools at the presented depth were considerably similar.
695 This disparity suggests that while users may have recognized
696 the functional effectiveness, aspects such as comfort or mental
697 load may have negatively influenced their preference. Many
698 participants perceived CDHandPos was “too heavy” (P15),
699 “much slower than my actual hand motion” (P3), and “wasn’t
700 really following my arm” (P1). The disconnection between the
701 ray and the hand may have significantly affected participants’
702 perception of control.

703 CDRayRev proved to be the most effective technique
704 for high-precision tasks, offering strong perceived accuracy,
705 preference, and stability. Despite its departure from con-
706 ventional raycasting, its converging behavior contributed to a
707 strong sense of intuitiveness. CDRayDir was better suited
708 for moderate-precision tasks where speed and ease of control
709 were prioritized. In contrast, CDHandPos revealed a trade-off
710 between perceived accuracy and user comfort, caused by a
711 disconnect between hand motion and pointer response. These
712 findings emphasize the importance of aligning interaction
713 techniques to task demands. Overall, CDRayRev appears most
714 appropriate for fine manipulation, while CDRayDir may be
715 beneficial for general-purpose contexts.

716 *3) Limitations & Future Works:* Although ForceCtrl
717 demonstrated clear benefits in both objective performance and
718 subjective responses, there remains room for refinement. In
719 our implementation, higher force levels (e.g., “3:Moderate”
720 and “7:Very Strong”) were chosen to ensure stable sensing, but
721 repeatedly exerting strong force may be physically demanding.
722 While users would likely activate high-precision states less

723 frequently in practice, increasing force detection sensitivity
724 could improve responsiveness and user experience. Likewise,
725 enhancing force classification accuracy and speed would help
726 reduce latency in state transitions. Although this study focused
727 on experienced hand-raycasting users, the system is scalable to
728 broader populations due to its controller-free design, familiar
729 gestures, and minimal cognitive effort. In addition, we focused
730 on user-defined force input rather than gesture recognition, but
731 the wristband's potential for out-of-sight interaction could be
732 further explored in future work.

733 While we adopted a discrete state approach to balance
734 usability and interaction clarity, future work may explore
735 hybrid strategies that combine continuous control of CD gain
736 with discrete state transitions. Such an approach could offer
737 finer-grained precision while preserving distinct interaction
738 phases, potentially enhancing user performance in complex
739 spatial tasks. Incorporating real-time visualization of force
740 classification could also assist users in maintaining more con-
741 sistent control. A proper visual feedback will reduce cognitive
742 effort [68] and improve performance especially during high-
743 precision tasks. Finally, exploring use cases could further
744 demonstrate the system's practical utility. We anticipate our
745 system to support high-precision tasks in dense 3D environ-
746 ments, such as those found in advanced AR/VR applications.

747 VII. CONCLUSION

748 We introduced ForceCtrl, a novel 3D hand raycasting tech-
749 nique that enables users to control pointing precision through
750 user-defined pinch force. By applying CD gain directly to
751 the ray, the system offers a target-agnostic, bare-hand method
752 for refining pointing accuracy. Our evaluation demonstrated
753 that ForceCtrl significantly improves pointing performance,
754 particularly for small and distant targets. We also proposed and
755 compared three CD gain strategies, highlighting the benefits
756 of ray convergence in high-difficulty tasks. These findings
757 underscore the potential of personalized, force-based input as
758 a scalable and effective modality for precise 3D interaction.
759 Future work may explore more stable sensing, broader task
760 generalization, and integration with multimodal feedback to
761 further expand the utility of ForceCtrl. We believe this research
762 contributes to advancing 3D interface design for professional
763 and immersive contexts that involve complex visual data and
764 demand high pointing precision.

765 REFERENCES

- [1] D. Yu, Q. Zhou, J. Newn, T. Dingler, E. Veloso, and J. Goncalves, "Fully-occluded target selection in virtual reality," *IEEE transactions on visualization and computer graphics*, vol. 26, no. 12, pp. 3402–3413, 2020.
- [2] F. Zhu, L. Sidenmark, M. Sousa, and T. Grossman, "Pinchlens: Applying spatial magnification and adaptive control-display gain for precise selection in virtual reality," in *IEEE International Symposium on Mixed and Augmented Reality*. IEEE Computer Society, 2023, pp. 1221–1230.
- [3] M. R. Mine, "Virtual environment interaction techniques," *UNC Chapel Hill CS Dept*, 1995.
- [4] G. De Haan, M. Koutek, and F. H. Post, "Intenselect: Using dynamic object rating for assisting 3d object selection." in *Ipt/egve*, 2005, pp. 201–209.
- [5] A. U. Batmaz and W. Stuerzlinger, "Effects of 3d rotational jitter and selection methods on 3d pointing tasks," in *IEEE Conference on Virtual Reality and 3D User Interfaces*, 2019, pp. 1687–1692.
- [6] S. V. Babu, H.-C. Huang, R. J. Teather, and J.-H. Chuang, "Comparing the fidelity of contemporary pointing with controller interactions on performance of personal space target selection," in *IEEE International Symposium on Mixed and Augmented Reality*, 2022, pp. 404–413.
- [7] Y. Lu, C. Yu, and Y. Shi, "Investigating bubble mechanism for ray-casting to improve 3d target acquisition in virtual reality," in *IEEE Conference on virtual reality and 3D user interfaces*. IEEE, 2020, pp. 35–43.
- [8] M. Krüger, T. Gerrits, T. Römer, T. Kuhlen, and T. Weissker, "Intenselect+: Enhancing score-based selection in virtual reality," *IEEE Transactions on Visualization and Computer Graphics*, 2024.
- [9] D. Yu, H.-N. Liang, X. Lu, K. Fan, and B. Ens, "Modeling endpoint distribution of pointing selection tasks in virtual reality environments," *ACM Transactions on Graphics*, vol. 38, no. 6, pp. 1–13, 2019.
- [10] R. Henrikson, T. Grossman, S. Trowbridge, D. Wigdor, and H. Benko, "Hand-coupled kinematic template matching: A prediction model for ray pointing in vr," in *Proceedings of the CHI Conference on Human Factors in Computing Systems*, 2020, pp. 1–14.
- [11] W. Xu, Y. Wei, X. Hu, W. Stuerzlinger, Y. Wang, and H.-N. Liang, "Predicting ray pointer landing poses in vr using multimodal lstm-based neural networks," in *2025 IEEE Conference Virtual Reality and 3D User Interfaces (VR)*, 2025, pp. 93–103.
- [12] M. N. Lystbæk, T. Mikkelsen, R. Krisztandl, E. J. Gonzalez, M. Gonzalez-Franco, H. Gellersen, and K. Pfeuffer, "Hands-on, hands-off: Gaze-assisted bimanual 3d interaction," in *Proceedings of the 37th Annual ACM Symposium on User Interface Software and Technology*, 2024, pp. 1–12.
- [13] J. Kim, S. Park, Q. Zhou, M. Gonzalez-Franco, J. Lee, and K. Pfeuffer, "Pinchcatcher: Enabling multi-selection for gaze+pinch," in *Proceedings of the 2025 CHI Conference on Human Factors in Computing Systems*, 2025.
- [14] I. Chatterjee, R. Xiao, and C. Harrison, "Gaze+ gesture: Expressive, precise and targeted free-space interactions," in *Proceedings of the 2015 ACM on international conference on multimodal interaction*, 2015, pp. 131–138.
- [15] F. L. Luro and V. Sundstedt, "A comparative study of eye tracking and hand controller for aiming tasks in virtual reality," in *Proceedings of the 11th ACM Symposium on eye tracking research & applications*, 2019, pp. 1–9.
- [16] L. Besançon, M. Ammi, and T. Isenberg, "Pressure-based gain factor control for mobile 3d interaction using locally-coupled devices," in *Proceedings of the CHI Conference on Human Factors in Computing Systems*, 2017, pp. 1831–1842.
- [17] C. Corsten, M. Lahaye, J. Borchers, and S. Voelker, "Forceray: Extending thumb reach via force input stabilizes device grip for mobile touch input," in *Proceedings of the CHI Conference on Human Factors in Computing Systems*, 2019, pp. 1–12.
- [18] G. A. Borg, "Psychophysical bases of perceived exertion." *Medicine & science in sports & exercise*, 1982.
- [19] W. A. König, J. Gerken, S. Dierdorf, and H. Reiterer, "Adaptive pointing—design and evaluation of a precision enhancing technique for absolute pointing devices," in *Human-Computer Interaction—INTERACT 2009: 12th IFIP TC 13 International Conference, Uppsala, Sweden, August 24–28, 2009, Proceedings, Part I 12*. Springer, 2009, pp. 658–671.
- [20] D. Bowman, C. Wingrave, J. Campbell, and V. Ly, "Using pinch gloves for both natural and abstract interaction techniques in virtual environments," *Proceedings of HCI International*, 2001.
- [21] D. Wolf, J. Gugenheimer, M. Combosch, and E. Rukzio, "Understanding the heisenberg effect of spatial interaction: A selection induced error for spatially tracked input devices," in *Proceedings of the CHI Conference on Human Factors in Computing Systems*, 2020, pp. 1–10.
- [22] S. Frees, G. D. Kessler, and E. Kay, "Prism interaction for enhancing control in immersive virtual environments," *ACM Transactions on Computer-Human Interaction*, vol. 14, no. 1, pp. 2–es, 2007.
- [23] A. Steed, "Towards a general model for selection in virtual environments," in *3D User Interfaces*. IEEE, 2006, pp. 103–110.
- [24] L. Vanacken, T. Grossman, and K. Coninx, "Exploring the effects of environment density and target visibility on object selection in 3d virtual environments," in *IEEE symposium on 3D user interfaces*. IEEE, 2007.
- [25] T. Grossman and R. Balakrishnan, "The design and evaluation of selection techniques for 3d volumetric displays," in *Proceedings of the 19th annual ACM symposium on User interface software and technology*, 2006, pp. 3–12.
- [26] G. Ren and E. O'Neill, "3d selection with freehand gesture," *Computers & Graphics*, vol. 37, no. 3, pp. 101–120, 2013.

[27] M. Baloup, T. Pietrzak, and G. Casiez, "Raycursor: A 3d pointing facilitation technique based on raycasting," in *Proceedings of the 2019 CHI Conference on Human Factors in Computing Systems*, 2019, pp. 1–12.

[28] R. Shi, J. Zhang, Y. Yue, L. Yu, and H.-N. Liang, "Exploration of bare-hand mid-air pointing selection techniques for dense virtual reality environments," in *Extended Abstracts of the CHI Conference on Human Factors in Computing Systems*, 2023, pp. 1–7.

[29] G. Casiez, D. Vogel, R. Balakrishnan, and A. Cockburn, "The impact of control-display gain on user performance in pointing tasks," *Human-computer interaction*, vol. 23, no. 3, pp. 215–250, 2008.

[30] I. Poupyrev, M. Billinghurst, S. Weghorst, and T. Ichikawa, "The go-go interaction technique: non-linear mapping for direct manipulation in vr," in *Proceedings of the 9th annual ACM symposium on User interface software and technology*, 1996, pp. 79–80.

[31] S. Frees and G. D. Kessler, "Precise and rapid interaction through scaled manipulation in immersive virtual environments," in *IEEE Proceedings. Virtual Reality*. IEEE, 2005, pp. 99–106.

[32] F. Rodrigues, A. Giovannelli, L. Pavanatto, H. Miao, J. C. de Oliveira, and D. A. Bowman, "Amp-it and wisdom: Improving 3d manipulation for high-precision tasks in virtual reality," in *IEEE International Symposium on Mixed and Augmented Reality*, 2023, pp. 303–311.

[33] M. Nancel, E. Pietriga, O. Chapuis, and M. Beaudouin-Lafon, "Mid-air pointing on ultra-walls," *ACM Transactions on Computer-Human Interaction*, vol. 22, no. 5, pp. 1–62, 2015.

[34] D. Vogel and R. Balakrishnan, "Distant freehand pointing and clicking on very large, high resolution displays," in *Proceedings of the 18th annual ACM symposium on User interface software and technology*, 2005, pp. 33–42.

[35] C. Forlines, D. Vogel, and R. Balakrishnan, "Hybridpointing: fluid switching between absolute and relative pointing with a direct input device," in *Proceedings of the 19th annual ACM symposium on User interface software and technology*, 2006, pp. 211–220.

[36] M. Nancel, O. Chapuis, E. Pietriga, X.-D. Yang, P. P. Irani, and M. Beaudouin-Lafon, "High-precision pointing on large wall displays using small handheld devices," in *Proceedings of the SIGCHI Conference on Human Factors in Computing Systems*, 2013, pp. 831–840.

[37] M. Kytö, B. Ens, T. Piumsomboon, G. A. Lee, and M. Billinghurst, "Pinpointing: Precise head-and eye-based target selection for augmented reality," in *Proceedings of the 2018 CHI Conference on Human Factors in Computing Systems*, 2018, pp. 1–14.

[38] H.-S. Yeo, J. Lee, H.-i. Kim, A. Gupta, A. Bianchi, D. Vogel, H. Koike, W. Woo, and A. Quigley, "Wrist: Watch-ring interaction and sensing technique for wrist gestures and macro-micro pointing," in *Proceedings of the 21st International Conference on Human-Computer Interaction with Mobile Devices and Services*, 2019, pp. 1–15.

[39] C. Andujar and F. Argelaguet, "Anisomorphic ray-casting manipulation for interacting with 2d guis," *Computers & Graphics*, vol. 31, no. 1, pp. 15–25, 2007.

[40] H. Ro, S. Chae, I. Kim, J. Byun, Y. Yang, Y. Park, and T. Han, "A dynamic depth-variable ray-casting interface for object manipulation in ar environments," in *IEEE International Conference on Systems, Man, and Cybernetics*, 2017, pp. 2873–2878.

[41] Y. Jang, I. Jeon, T.-K. Kim, and W. Woo, "Metaphoric hand gestures for orientation-aware vr object manipulation with an egocentric viewpoint," *IEEE Transactions on Human-Machine Systems*, vol. 47, no. 1, pp. 113–127, 2016.

[42] Y. Yan, C. Yu, X. Ma, X. Yi, K. Sun, and Y. Shi, "Virtualgrasp: Leveraging experience of interacting with physical objects to facilitate digital object retrieval," in *Proceedings of the 2018 CHI conference on human factors in computing systems*, 2018, pp. 1–13.

[43] S. Pei, A. Chen, J. Lee, and Y. Zhang, "Hand interfaces: Using hands to imitate objects in ar/vr for expressive interactions," in *Proceedings of the 2022 CHI conference on human factors in computing systems*, 2022, pp. 1–16.

[44] H. B. Surale, F. Matulic, and D. Vogel, "Experimental analysis of barehand mid-air mode-switching techniques in virtual reality," in *Proceedings of the CHI conference on human factors in computing systems*, 2019, pp. 1–14.

[45] Z. Song, J. J. Dudley, and P. O. Kristensson, "Efficient special character entry on a virtual keyboard by hand gesture-based mode switching," in *2022 IEEE International Symposium on Mixed and Augmented Reality*. IEEE, 2022, pp. 864–871.

[46] A. K. Mutasim, A. U. Batmaz, and W. Stuerzlinger, "Pinch, click, or dwell: Comparing different selection techniques for eye-gaze-based pointing in virtual reality," in *AcM symposium on eye tracking research and applications*, 2021, pp. 1–7.

[47] A. M. Feit, S. Williams, A. Toledo, A. Paradiso, H. Kulkarni, S. Kane, and M. R. Morris, "Toward everyday gaze input: Accuracy and precision of eye tracking and implications for design," in *Proceedings of the 2017 CHI conference on human factors in computing systems*, 2017, pp. 1118–1130.

[48] R. J. Jacob, "What you look at is what you get: eye movement-based interaction techniques," in *Proceedings of the SIGCHI conference on Human factors in computing systems*, 1990, pp. 11–18.

[49] R. Shi, Y. Wei, X. Hu, Y. Liu, Y. Yue, L. Yu, and H.-N. Liang, "Experimental analysis of freehand multi-object selection techniques in virtual reality head-mounted displays," *Proceedings of the ACM on Human-Computer Interaction*, vol. 8, no. ISS, pp. 93–111, 2024.

[50] J. Kim, Y. Zhang, and S. H. Yoon, "T2iray: Design of thumb-to-index based indirect pointing for continuous and robust ar/vr input," in *Proceedings of the 2025 CHI Conference on Human Factors in Computing Systems*, 2025, pp. 1–16.

[51] R. Shi, Y. Wei, X. Qin, P. Hui, and H.-N. Liang, "Exploring gaze-assisted and hand-based region selection in augmented reality," *Proceedings of the ACM on Human-Computer Interaction*, vol. 7, no. ETRA, pp. 1–19, 2023.

[52] K. Pfeuffer, J. Obernolte, F. Dietz, V. Mäkelä, L. Sidenmark, P. Mankov, M. Pakanen, and F. Alt, "Palmgazer: Unimanual eye-hand menus in augmented reality," in *Proceedings of the 2023 ACM Symposium on Spatial User Interaction*, 2023, pp. 1–12.

[53] T. J. Dube, Y. Ren, H. Limerick, I. S. MacKenzie, and A. S. Arif, "Push, tap, dwell, and pinch: Evaluation of four mid-air selection methods augmented with ultrasonic haptic feedback," *Proceedings of the ACM on Human-Computer Interaction*, vol. 6, no. ISS, pp. 207–225, 2022.

[54] S. Y. Oh, B. Yoon, H.-i. Kim, and W. Woo, "Finger contact in gesture interaction improves time-domain input accuracy in hmd-based augmented reality," in *Extended Abstracts of the 2020 CHI Conference on Human Factors in Computing Systems*, 2020, pp. 1–8.

[55] U. Wagner, A. A. Jacobsen, T. Feuchtner, H. Gellersen, and K. Pfeuffer, "Eye-hand movement of objects in near space," in *Companion Proceedings of the 2024 Conference on Interactive Surfaces and Spaces*, 2024, pp. 18–21.

[56] V. Vuibert, W. Stuerzlinger, and J. R. Cooperstock, "Evaluation of docking task performance using mid-air interaction techniques," in *Proceedings of the 3rd ACM Symposium on Spatial User Interaction*, 2015, pp. 44–52.

[57] E. Velloso, J. Turner, J. Alexander, A. Bulling, and H. Gellersen, "An empirical investigation of gaze selection in mid-air gestural 3d manipulation," in *Human-Computer Interaction–INTERACT 2015: 15th IFIP TC 13 International Conference, Bamberg, Germany, September 14–18, 2015, Proceedings, Part II 15*. Springer, 2015, pp. 315–330.

[58] P. C. Gloumeau, W. Stuerzlinger, and J. Han, "Pinnpivot: Object manipulation using pins in immersive virtual environments," *IEEE transactions on visualization and computer graphics*, vol. 27, no. 4, pp. 2488–2494, 2020.

[59] Y.-J. Huang, T. Fujiwara, Y.-X. Lin, W.-C. Lin, and K.-L. Ma, "A gesture system for graph visualization in virtual reality environments," in *2017 ieee pacific visualization symposium (pacificvis)*. IEEE, 2017, pp. 41–45.

[60] K. Pfeuffer, B. Mayer, D. Mardanbegi, and H. Gellersen, "Gaze+ pinch interaction in virtual reality," in *Proceedings of the 5th symposium on spatial user interaction*, 2017, pp. 99–108.

[61] M. Schmitz, S. Günther, D. Schön, and F. Müller, "Squeezee-feely: Investigating lateral thumb-index pinching as an input modality," in *Proceedings of the 2022 CHI Conference on Human Factors in Computing Systems*, 2022, pp. 1–15.

[62] C. Corsten, S. Voelker, A. Link, and J. Borchers, "Use the force picker, luke: Space-efficient value input on force-sensitive mobile touchscreens," in *Proceedings of the CHI Conference on Human Factors in Computing Systems*, 2018, pp. 1–12.

[63] E. W. Pedersen and K. Hornbæk, "Expressive touch: Studying tapping force on tabletops," in *Proceedings of the SIGCHI Conference on Human Factors in Computing Systems*, 2014, pp. 421–430.

[64] G. Ramos, M. Boulos, and R. Balakrishnan, "Pressure widgets," in *Proceedings of the SIGCHI conference on Human factors in computing systems*, 2004, pp. 487–494.

[65] A. Goguey, S. Malacria, and C. Gutwin, "Improving discoverability and expert performance in force-sensitive text selection for touch devices with mode gauges," in *Proceedings of the 2018 chi conference on human factors in computing systems*, 2018, pp. 1–12.

[66] G. Ramos and R. Balakrishnan, "Zliding: fluid zooming and sliding for high precision parameter manipulation," in *Proceedings of the 18th*

1011 annual ACM symposium on User interface software and technology, 1088
1012 2005, pp. 143–152.

1013 [67] X. Ren, J. Yin, S. Zhao, and Y. Li, “The adaptive hybrid cursor: A 1089
1014 pressure-based target selection technique for pen-based user interfaces,” 1090
1015 in *Human-Computer Interaction–INTERACT 2007: 11th IFIP TC 13* 1091
1016 *International Conference, Rio de Janeiro, Brazil, September 10–14, 1092*
1017 *2007, Proceedings, Part I 11*. Springer, 2007, pp. 310–323.

1018 [68] H.-i. Kim, B. Yoon, S. Y. Oh, and W. Woo, “Visualizing hand force 1093
1019 with wearable muscle sensing for enhanced mixed reality remote collaboration,” 1094
1020 *IEEE Transactions on Visualization and Computer Graphics*, 2023.

1021 [69] Y. Zhang, B. Liang, B. Chen, P. M. Torrens, S. F. Atashzar, D. Lin, and 1095
1022 Q. Sun, “Force-aware interface via electromyography for natural vr/ar 1096
1023 interaction,” *ACM Transactions on Graphics (TOG)*, vol. 41, no. 6, pp. 1–18, 2022.

1024 [70] T. S. Saponas, D. S. Tan, D. Morris, and R. Balakrishnan, “Demon- 1097
1025 strating the feasibility of using forearm electromyography for muscle- 1098
1026 computer interfaces,” in *Proceedings of the SIGCHI conference on 1099
1027 human factors in computing systems*, 2008, pp. 515–524.

1028 [71] F. Haque, M. Nancel, and D. Vogel, “Myopoint: Pointing and clicking 1100
1029 using forearm mounted electromyography and inertial motion sensors,” 1101
1030 in *Proceedings of the 33rd Annual ACM Conference on Human Factors 1102*
1031 in Computing Systems, 2015, pp. 3653–3656.

1032 [72] Y. Garnica Bonome, A. González Mondéjar, R. Cherullo de Oliveira, 1103
1033 E. de Albuquerque, and A. Raposo, “Design and assessment of two 1104
1034 handling interaction techniques for 3d virtual objects using the myo 1105
1035 armband,” in *Virtual, Augmented and Mixed Reality: Interaction, 1106
1036 Navigation, Visualization, Embodiment, and Simulation: 10th International 1107
1037 Conference, VAMR 2018, Held as Part of HCI International 2018, Las 1108
1038 Vegas, NV, USA, July 15–20, 2018, Proceedings, Part I 10*. Springer, 1109
1039 2018, pp. 30–42.

1040 [73] E. Eddy, E. J. Scheme, and S. Bateman, “A framework and call to action 1110
1041 for the future development of emg-based input in hci,” in *Proceedings 1111*
1042 of the 2023 CHI Conference on Human Factors in Computing Systems, 1112
1043 2023, pp. 1–23.

1044 [74] C. Choi, S. Kwon, W. Park, H.-d. Lee, and J. Kim, “Real-time pinch 1113
1045 force estimation by surface electromyography using an artificial neural 1114
1046 network,” *Medical engineering & physics*, vol. 32, no. 5, pp. 429–436, 1115
1047 2010.

1048 [75] V. Becker, P. Oldrati, L. Barrios, and G. Sörös, “Touchsense: classifying 1116
1049 finger touches and measuring their force with an electromyography 1117
1050 armband,” in *Proceedings of the 2018 ACM International Symposium 1118*
1051 on Wearable Computers, 2018, pp. 1–8.

1052 [76] F. Leone, C. Gentile, A. L. Ciancio, E. Gruppioni, A. Davalli, R. Sac- 1119
1053 chetti, E. Guglielmelli, and L. Zollo, “Simultaneous semg classification 1120
1054 of hand/wrist gestures and forces,” *Frontiers in neurorobotics*, vol. 13, 1121
1055 p. 42, 2019.

1056 [77] S. Hickman, R. Alba-Flores, and M. Ahad, “Emg based classification 1122
1057 of percentage of maximum voluntary contraction using artificial neural 1123
1058 networks,” in *2014 IEEE Dallas Circuits and Systems Conference 1124*
1059 (DCAS). IEEE, 2014, pp. 1–4.

1060 [78] Q. Zengyu, Z. Lu, L. Zhoujie, C. Yingjie, C. Shaoxiong, H. Baizheng, 1125
1061 and Y. Ligang, “A simultaneous gesture classification and force estimation 1126
1062 strategy based on wearable a-mode ultrasound and cascade model,” 1127
1063 *IEEE Transactions on Neural Systems and Rehabilitation Engineering*, 1128
1064 vol. 30, pp. 2301–2311, 2022.

1065 [79] K. W. Li and R. Yu, “Assessment of grip force and subjective hand force 1129
1066 exertion under handedness and postural conditions,” *Applied ergonomics*, 1130
1067 vol. 42, no. 6, pp. 929–933, 2011.

1068 [80] R. W. McGorry, J.-H. Lin, P. G. Dempsey, and J. S. Casey, “Accuracy 1131
1069 of the borg cr10 scale for estimating grip forces associated with hand 1132
1070 tool tasks,” *Journal of Occupational and Environmental Hygiene*, vol. 7, 1133
1071 no. 5, pp. 298–306, 2010.

1072 [81] T. Chen and C. Guestrin, “XGBoost: A scalable tree boosting system,” 1134
1073 in *Proceedings of the 22nd ACM SIGKDD International Conference on 1135*
1074 *Knowledge Discovery and Data Mining*, 2016, pp. 785–794.

1075 [82] A. R. Tilley *et al.*, *The measure of man and woman: human factors in 1136*
1076 *design*. John Wiley & Sons, 2001.

1077 [83] F. Bérard, G. Wang, and J. R. Cooperstock, “On the limits of the human 1137
1078 motor control precision: the search for a device’s human resolution,” 1138
1079 in *Human-Computer Interaction–INTERACT 2011: 13th IFIP TC 13 1139*
1080 *International Conference, Lisbon, Portugal, September 5–9, 2011, Pro- 1140*
1081 ceedings, Part II 13. Springer, 2011, pp. 107–122.

1082 [84] D. A. Bowman and L. F. Hodges, “An evaluation of techniques for 1141
1083 grabbing and manipulating remote objects in immersive virtual environments,” 1142
1084 in *Proceedings of the symposium on Interactive 3D graphics*, 1143
1085 1997, pp. 35–ff.

1086 [85] S. G. Hart, “Nasa-task load index (nasa-tlx); 20 years later,” in *Pro- 1144*
1087 ceedings of the human factors and ergonomics society annual meeting, 1145
1088 vol. 50, no. 9. Sage publications Sage CA: Los Angeles, CA, 2006, 1146
1089 pp. 904–908.

1090 [86] J. O. Wobbrock, L. Findlater, D. Gergle, and J. J. Higgins, “The aligned 1147
1091 rank transform for nonparametric factorial analyses using only anova 1148
1092 procedures,” in *Proceedings of the SIGCHI conference on human factors 1149*
1093 in computing systems, 2011, pp. 143–146.

1094

VIII. BIOGRAPHY SECTION

Seo Young Oh is currently pursuing a Ph.D. degree with the Graduate School of Culture Technology (GSCT), Korea Advanced Institute of Science and Technology (KAIST), Daejeon, Korea. She investigates 3D hand interactions for augmented reality as part of the Ubiquitous Virtual Reality (UVR) Lab under Prof. Woontack Woo. She is focusing on enhancing the accuracy of 3D interactions for professional scenarios in augmented reality. She received her M.S. from GSCT, KAIST (2020) and B.S. in Mechanical Engineering from KAIST (2014).

Junghoon Seo is currently pursuing a Master’s degree at GSCT, KAIST, Daejeon, Korea, where he is a member of the Human-centered Interactive Technologies Lab (HCI Tech Lab) under the supervision of Prof. Sang Ho Yoon. His research interests include intellectual user interface, computer vision, machine learning, and remote sensing. He received his B.S. degree in Electrical Engineering and Computer Science from Gwangju Institute of Science and Technology (GIST), Gwangju, Korea, in 2021.

Juyoung Lee is pursuing his Ph.D. at GSCT, KAIST, Daejeon, Korea. As a member of the UVR Lab under Prof. Woontack Woo, he explores novel interaction techniques for AR. His research interests include smartglasses interaction, gestural and subtle interaction, wearable computing, and augmented reality. Mr. Lee received his M.S. from GSCT, KAIST (2017) and B.S. in Electrical & Electronic Engineering from Yonsei University (2014).

Boram Yoon is a senior researcher at the KI-ITC Augmented Reality Research Center (ARRC), KAIST, Daejeon, Korea. Her research focuses on virtual avatar embodiment and user experience for XR remote collaboration and Metaverse. She received her Ph.D. and M.S. degrees from GSCT, KAIST, and B.S. in Computer Science and Engineering from Ewha Womans University, Seoul, Korea.

Sang Ho Yoon is an associate professor in GSCT, KAIST. He leads the HCI Tech Lab. His research focuses on developing natural user interactions that address physical, mental, and social barriers with novel haptic interfaces and sensing techniques. He was a principal engineer at Samsung Research and a research engineer at Microsoft Applied Sciences Lab. He received Ph.D. from Purdue University, and M.S. and B.S. from Carnegie Mellon University.

Woontack Woo is a professor of GSCT, KAIST, Daejeon, Korea. He is also the director of both the CT Research Institute and the KI-ITC ARRC, KAIST. In 2001, he coined the term ‘Ubiquitous Virtual Reality (UVR)’ and started the UVR Lab, GIST, Gwangju, Korea. The main theme of his research is to realize augmented humans, augmented cities, and even augmented societies by implementing Ubiquitous VR in smart spaces.

Authorized licensed use limited to: Korea Advanced Inst of Science & Tech - KAIST. Downloaded on February 05, 2026 at 10:23:07 UTC from IEEE Xplore. Restrictions apply.
© 2025 IEEE. All rights reserved, including rights for text and data mining and training of artificial intelligence and similar technologies. Personal use is permitted,

but republication/redistribution requires IEEE permission. See <https://www.ieee.org/publications/rights/index.html> for more information.